

Gamma and neutron dose rate measurements around the KATANA water activation loop at JSI TRIGA reactor

Domen Kotnik^{1,*}, Julijan Peric^{1,2}, Domen Govekar^{1,2}, and Igor Lengar¹

¹Reactor Physics Department, Jožef Stefan Institute, Slovenia

²Faculty of Mathematics and Physics, University of Ljubljana, Slovenia

(*) domen.kotnik@ijs.si

Abstract— KATANA water activation facility, which serves as a well-defined high-energy gamma and neutron source, has been successfully constructed at JSI TRIGA reactor at the end of 2023. During the commissioning phase γ and neutron dose rate measurements were conducted around the KATANA to create a comprehensive dose rate map under steady-state reactor operation with activated water flowing throughout the circuit. Dose rates, quantified as dose rate equivalents of $H^*(10)/\text{time}$, were measured using a certified neutron probe and two γ detectors. The peak γ dose rate observed was up to 5 mSv/h at the close vicinity of the main observation part of the circuit (Snail head), with neutron contributions markedly lower, by more than three orders of magnitude. Due to these elevated dose rates, the experimental zone within the concrete walls has been designated as a red zone, subject to stringent access restrictions. Outside the labyrinth, however, the dose rates remained below the limit of 10 $\mu\text{Sv/h}$, indicating no need for additional shielding. Experimental data were furtherly compared with the computational results using a simplified convectional method excluding detailed fluid dynamics. C/E comparison showed that the gamma dose rates were underestimated by a factor of 2–5, while neutron dose rates near the source (Snail No. 1) were overestimated by a factor of 1.8. These findings highlight the complexity of water activation analysis at KATANA and the need for accurate modelling. Future work should incorporate advanced, state-of-the-art fluid activation codes and refined experimental methods to increase precision and support benchmark-quality experiments.

Keywords —dose field measurements, N16, KATANA, water activation, Fusion, ITER.

I. INTRODUCTION

WATER as a primary coolant will play an important role in the performance of fusion reactors, as it causes an ionising radiation field throughout the facility after its irradiation and activation and requires improved shielding for instrumentation and personnel. The activation of water consists primarily of the activation of oxygen, resulting in the generation of activated ^{16}N , ^{17}N and ^{19}O , which furtherly decay releasing high energy gammas and neutrons. The threshold energy for the primary water activation reaction, in particular, $^{16}\text{O}(n,p)^{16}\text{N}$, is

about 10.5 MeV. Consequently, neutrons in fusion reactors lead to a water activity approximately five orders of magnitude higher than in fission reactors of comparable power [1].

To support ITER [2][3], the KATANA irradiation facility [4][5][6], which utilises a closed-water activation loop, was successfully licenced, built and commissioned at the end of 2023 at the JSI TRIGA research reactor in Slovenia [7]. The KATANA serves as a well-defined and stable high-energy (6 MeV - 7 MeV) gamma and ~ 1 MeV neutron source [8]. Such a high-energy irradiation facility will enable various experiments based on water activation, e.g. shielding experiments using ITER-relevant materials, investigation of the response of detectors to high-energy γ radiation, investigation of short-lived moving radiation sources, integral cross-section measurements, dose rates and spectrum measurements, etc. The ultimate goal of KATANA is to perform benchmark-quality experiments, e.g. experimental validation of fluid activation codes (i.e. RSTM [9] [10], FLUNED [11], GammaFlow & ActiFlow [12]), and to establish itself as a reference facility for the calibration of high-energy γ detectors [13], which will significantly support the operation of ITER, DEMO [14] and other future water-cooled fusion reactors.

To ensure safe operational conditions, it is critical that dose rates within the reactor hall remain sufficiently low, i.e. below the prescribed limit value of 10 $\mu\text{Sv/h}$, during KATANA and full-power operation of the TRIGA reactor. The aim of this work is to create a comprehensive gamma and neutron dose rate map around KATANA facility under steady-state reactor operation with activated water flowing throughout the circuit by performing gamma and neutron dose rate measurements at multiple locations. In addition, an experimental data were furtherly compared with the computational results using a simplified convectional method excluding detailed fluid dynamics.

The paper is structured as follows: Section 2 presents a brief description of the KATANA irradiation facility, Section 3 presents the performed gamma and neutron dose rate measurements, and Section 4 presents the computational analysis and comparison with the experimental data.

II. KATANA WATER ACTIVATION LOOP

A. Water activation

The short-term activation of water consists primarily of the activation of oxygen isotopes by the reactions $^{16}\text{O}(n, p)^{16}\text{N}$, $^{17}\text{O}(n, p)^{17}\text{N}$ and $^{18}\text{O}(n, \gamma)^{19}\text{O}$ [15], with a very small contribution from the activation of dissolved gases, corrosion products and additives. Activated nitrogen and oxygen nuclides subsequently decay, releasing γ rays and neutrons with different energies. The (n,p) reactions on ^{16}O and ^{17}O are threshold reactions, while the (n, γ) reaction on ^{18}O already occurs at thermal energies. The most important water activation reactions and the corresponding decay properties are listed in Table I. The main contribution to the activity of water during operation is the activated isotope ^{16}N due to the high natural abundance of the isotope ^{16}O and high cross-section for the (n,p) reaction.

TABLE I
ACTIVATION PRODUCTS OF WATER [15].

Reaction	$t_{1/2}$ [s]	Major decay products	Threshold energy	Natural abundance
$^{16}\text{O}(n,p)^{16}\text{N}$	7.13	γ : 6.13 MeV (67 %)	~ 10.5 MeV	99.76 %
		γ : 7.12 MeV (5 %)		
		n: 0.38 MeV (35 %)		
$^{17}\text{O}(n,p)^{17}\text{N}$	4.17	γ : 0.87 MeV (3 %)	~ 9 MeV	0.04 %
		n: 1.17 MeV (53 %)		
		n: 1.70 MeV (7 %)		
$^{18}\text{O}(n,\gamma)^{19}\text{O}$	26.88	γ : 0.11 MeV (3 %)	< 1 eV	0.2 %
		γ : 0.20 MeV (96 %)		
		γ : 1.36 MeV (50 %)		
		γ : 1.44 MeV (3 %)		

B. KATANA irradiation facility

KATANA water circuit, schematically shown in Fig. 1, consists of a pipe loop that is partially inserted into the radial piercing port (RPP). The main components are the inner irradiation Snail, two outer observation Snails and transport pipes. All important components, sensors and instruments for controlling and operating the circuit, e.g. pump, valves, Coriolis flow metres, temperature and pressure sensors, etc., are located outside the RPP (shown in black). A three-way valve can be used to fully or partially adjust the water distribution between the primary (shown in red) and secondary loops (shown in blue), referred to as Configuration 1 and Configuration 2, respectively, further in the text. The primary loop is designed to achieve the fastest possible transport of activated water in order to achieve a high total activity of ^{16}N and ^{17}N within the outer observation part (i.e. outer Snail No. 1), resulting in a lower experimental uncertainty, e.g. for performing shielding experiments with ITER-relevant materials. The secondary loop (or so-called delay loop) extends the travel time of the activated water and favours a $^{16}\text{N}/^{19}\text{O}$ isotope ratio in favour of ^{19}O . The use of these two different circuit components, each optimised for its specific function, improves the overall performance and accuracy of the system. In addition, the loop branching also enables the investigation of more complex scenarios such as the simulation of the mixing of the activated water flow from different pipes and/or the investigation of leakage scenarios.

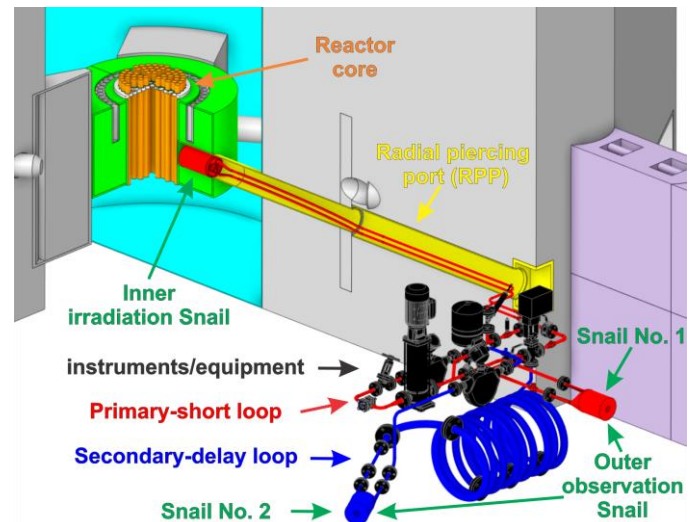


Fig. 1. Schematic of the KATANA water circuit only (adapted from [5]).

To minimise occupational radiation exposure inside the reactor hall, two special γ & neutron shielding plugs are used inside the RPP together with a 40 cm thick and 180 cm high concrete wall around the experimental area. The entire KATANA is controlled and monitored via the control panel, located outside of the labyrinth-shaped concrete wall. A fully constructed and commissioned KATANA facility is shown in Fig. 2.

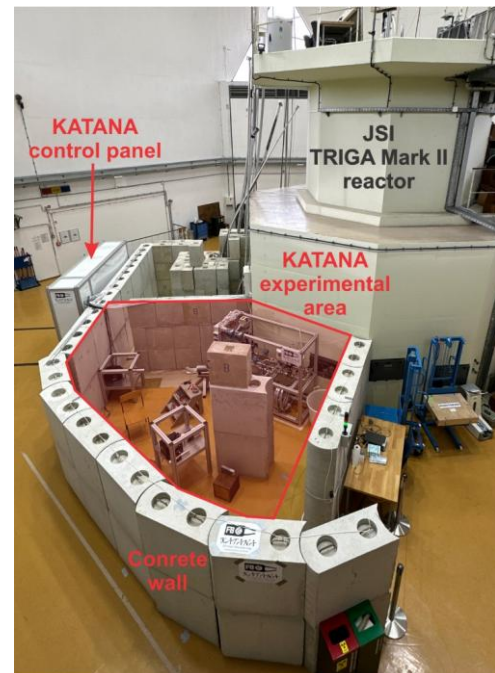


Fig. 2. Constructed and commissioned KATANA facility at JSI TRIGA research reactor (figure taken from [5]).

III. DOSE RATE MEASUREMENT

During the commissioning phase, and with a focus on safety, γ and neutron dose rate measurements were conducted around the KATANA circuit (within the experimental area enclosed by concrete walls) and across the reactor hall to create a comprehensive dose rate map under steady-state reactor operation (250 kW) with activated water flowing throughout the circuit (flow rate 0.4 L/s). Dose rates, quantified as dose rate

equivalents of $H^*(10)/\text{time}$, were measured using a certified neutron probe (Berthold LB 6411) and two γ detectors: a pressurized ionization chamber (Fluke Victoreen 451P-DE-SI-RYR) and a scintillator probe (Automess 6150AD-b/H). All three detectors, with the reported uncertainty of 25 %, are shown at the bottom left side of Fig. 3.

A total of 21 measurement positions (MPs), as shown in Fig.3, were strategically selected to characterize dose rate distributions at key locations around the KATANA facility. These included positions along the line of sight from the reactor pool plug (RPP), around the outer Snails No. 1 and 2, and at various points inside, outside, and at the entrance of the concrete shielding wall.

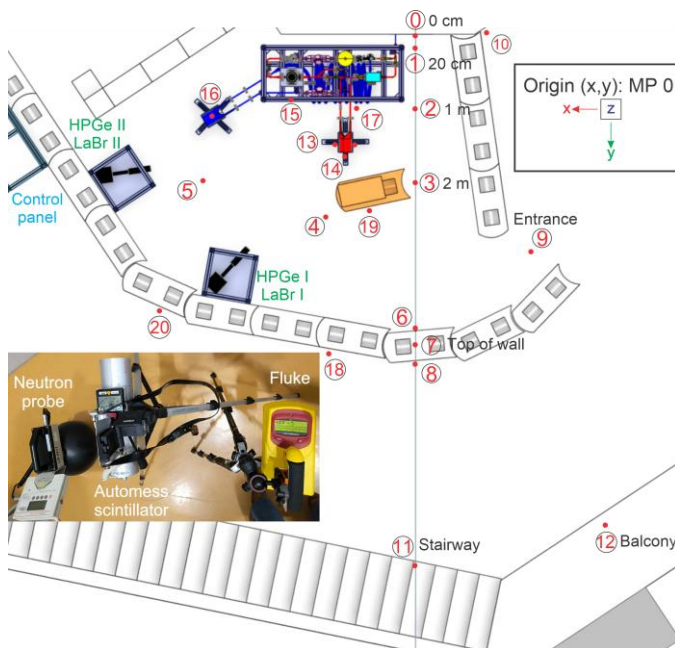


Fig. 3. 21 measurement positions for gamma and neutron dose rates around KATANA facility, covering both the shielded experimental area and selected locations in the reactor hall.

To capture peak dose rate values, most MPs were positioned at a height of 86 cm above the ground—corresponding to the vertical centreline of the RPP and the height of the primary circuit loop (Snail No. 1). Exceptions to this height included MP 17, located at the centre of the lower winding of the secondary loop inside the labyrinth wall, and several positions situated externally within the reactor hall: MP 7 (top of the concrete wall), MP 11 (stairway) and MP 12 (balcony).

Detailed spatial coordinates (x, y, z) of all MPs, with an associated positional uncertainty of ± 5 cm and the coordinate origin defined at ground level beneath MP 0, are provided in Table II, along with the corresponding dose rate measurements. Due to differing detector sensitivities across radiation field intensities, gamma dose rate measurements within the concrete shielding (MPs 0–7, 13–17, and 19) were performed using a Fluke ionization chamber. Conversely, dose rates at all other reactor hall locations (MPs 8–12, 18, and 20) were measured using an Automess scintillator probe, as indicated with an asterisk (*) in the tables.

As expected, the highest gamma dose rate—reaching up to 5 mSv/h—was measured near the outer Snail No. 1. The dose rate at the inlet side (MP 13) was almost 50 % higher than at the back side (MP 14), where the activity of the water is significantly reduced due to radioactive decay along its flow path through the Snail. A comparatively elevated gamma dose rate of 0.6 mSv/h was also recorded near the pump (MP 15), which can be attributed to the substantial volume of activated water in that region (approximately 4 litres).

Despite these localized peaks, all measurement positions located outside the experimental zone (i.e., beyond the concrete shielding wall) exhibited dose rates below the regulatory threshold of $10 \mu\text{Sv/h}$. The contribution of neutrons to the overall dose rate is more than three orders of magnitude lower than that of gamma radiation and is therefore considered negligible for the purposes of radiological assessment. Nevertheless, neutrons (originating from ^{17}N) are easily measured by using time dependent (^3He and BF_3) detectors and can be used to characterise KATANA characteristics [8].

TABLE II
EXPERIMENTAL AND CALCULATED DATA OF GAMMA AND NEUTRON DOSE RATE FOR 21 LOCATIONS AROUND KATANA (CONFIGURATION 1, 250 KW, FLOW RATE 0.4 L/S). CALCULATIONS (WITH C/E VALUES) CONSIDERED SINGLE AND DOUBLE SOURCE LOCATION OF ACTIVATED WATER.

LOCATION				SINGLE SOURCE (Snail no.1)						DOUBLE SOURCE (Snail no.1 + pump)			
				Experiment		Calculation		C/E		Calculation		C/E	
MP	X	Y	Z	γ	neutron	γ	neutron	γ	neutron	γ	neutron	γ	neutron
[/]	[cm]	[cm]	[cm]	[μ Sv/h]	[μ Sv/h]	[μ Sv/h]	[μ Sv/h]	[/]	[/]	[μ Sv/h]	[μ Sv/h]	[/]	[/]
0	0	0	0	132	11	7.2	3.47E-02	0.05	0.003	10.6	4.31E-02	0.08	0.004
1	0	20	1	30	9	10.1	4.83E-02	0.34	0.005	13.5	5.68E-02	0.45	0.006
2	0	100	2	120	0.8	22.6	9.07E-02	0.19	0.11	26.2	1.00E-01	0.22	0.13
3	0	200	3	50	0.5	8.3	2.54E-02	0.17	0.05	9.8	2.89E-02	0.20	0.06
4	-121	246	4	122	0.4	19.9	4.95E-02	0.16	0.12	22.9	5.71E-02	0.19	0.14
5	-286	197	5	54	0.1	6.2	2.82E-02	0.1	0.28	9.6	3.71E-02	0.18	0.37
6	0	398	6	3	0.2	0.7	4.36E-03	0.22	0.02	0.8	5.34E-03	0.26	0.03
7	0	418	7	2	0	0.2	1.27E-03	0.09	N/A	0.2	1.61E-03	0.12	N/A
8	0	444	8	0.4*	0	0.1	3.18E-04	0.29	N/A	0.1	4.29E-04	0.33	N/A
9	156	293	9	1.3*	0	0.2	1.28E-03	0.16	N/A	0.3	1.63E-03	0.22	N/A
10	96	-2	10	2.8*	0	0.9	1.00E-03	0.33	N/A	1.1	1.24E-03	0.41	N/A
11	0	714	11	1.7*	0	0.1	7.30E-04	0.04	N/A	0.3	1.37E-03	0.17	N/A
12	256	661	12	1.4*	0	0.0	5.49E-04	0.02	N/A	0.0	7.20E-04	0.03	N/A
13	-107	148	13	5000	3	1388.3	3.66	0.28	1.22	1397.7	3.68	0.28	1.23
14	-94	164	14	3400	2	1231.4	3.53	0.36	1.77	1236.8	3.54	0.36	1.77
15	-167	87	15	600	1.1	26.8	9.70E-02	0.04	0.09	109.1	2.34E-01	0.18	0.21
16	-273	111	16	90	0.3	7.5	3.41E-02	0.08	0.11	14.8	5.04E-02	0.16	0.17
17	-79	100	17	320	1.1	49.0	1.59E-01	0.15	0.14	56.0	1.74E-01	0.17	0.16
18	-116	430	18	0.6*	0	0.1	4.00E-04	0.06	N/A	0.2	6.01E-04	0.37	N/A
19	-62	237	19	9	0	5.8	9.23E-03	0.65	N/A	6.3	1.05E-02	0.70	N/A
20	-344	372	20	1.7*	0	0.5	7.71E-04	0.30	N/A	0.7	1.03E-03	0.42	N/A

Remarks: a) N/A: experimental value is 0. b) C/E values between 0.2 – 5 are highlighted.

c) Relative statistical uncertainty for all MP is below 2 %. d) All dose rate detectors have stated measurement uncertainties of 25 %.

e) γ dose rate measurements noted with the (*) were performed with the Automess scintillator detector (others with Fluke detector).

IV. COMPARISON OF COMPUTATIONAL AND EXPERIMENTAL DATA

A. Computational model

Experimental data described above were also compared with the computational results. To perform that, an MCNP model containing the TRIGA reactor core and the inner part of the KATANA structure, which was used for the calculation of the RR density profiles of ¹⁶N, ¹⁷N and ¹⁹O inside the inner irradiation Snail (see article [5]), was updated to include the outer part of the KATANA facility and the reactor hall. Once again, the detailed CAD model (schematically shown in Fig. 3) was simplified in order to be converted to the MCNP file using the GEOUNED [16] program.

In the second step, the source of activated water was defined, which is evenly distributed within the outer Snail No. 1, i.e. the main source of activated water for the primary loop - Configuration 1, without taking into account contribution of activated water from the rest of the circuit. The intensity of the source was determined based on the calculated saturated

activity values of ¹⁶N (7.01×10^7 Bq; 77.675 %), ¹⁷N (1.15×10^4 Bq; 0.017 %) and ¹⁹O (9.54×10^6 Bq; 22.307 %) inside the Snail No. 1 and taking into the account the dominant released γ rays and neutrons (see Table I).

The γ and neutron dose rate values were calculated as an ambient dose equivalent H*(10) by using flux-to-dose rate conversion factors (ICRP-21 [17] and NCRP-38 [18]).

B. Computational results: single source location

γ and neutron dose rates were calculated at selected twenty-one measurement positions (MP: 0 - 20) and on a global mesh area, i.e. meshtally, around the KATANA facility, providing a global dose field distribution and insight into the important streaming paths. Results of the global γ (top) and neutron (bottom) dose field distributions are presented in Fig. 4 respectively, in a horizontal cross-section view (XY plane) at the height of the centre of the outer Snail No. 1 (Z = 86.4cm). In addition, the contour lines have been added in red for better clarity. The maximum achieved γ and neutron dose rate inside the Snail No.1 are 6.7 mSv/h and 23.8 μ Sv/h, respectively, which are gradually decreased for more than four orders of

magnitude throughout the area. The main factor is the radial (R^2) dependence on the distance from the source, whereby the surrounding shielding concrete wall further decreases the radiation.

From the safety point of view, the dose rate outside the wall, i.e. outside the experimental area, is well below the limit value of $10 \mu\text{Sv/h}$, whereby the contribution of the neutrons to the total dose rate is negligible and more than 2 orders of magnitude smaller than that from gammas. However, some unique streaming characteristics can be observed between them, due to the nature of the interaction between gammas and neutrons with matter. Specifically, for gammas, streaming paths ("rays") with higher dose rate values are observed from the concrete shielding wall onwards. The reason for this phenomenon is the extra empty space (can be seen in Fig. 2. and Fig. 3) at the top of each shielding block that is used for handling. The effect is even more pronounced because the source (Snail No. 1), located at a height of 86.4 cm, is nearly aligned with the top of the first row of the shielding wall (90 cm). This effect was not known before the analysis. However, it was unintentionally taken into account when selecting the locations of MP 18 and MP 20, which were chosen based on the highest measured γ dose rate in the vicinity of the corresponding location, i.e. the tallies (spheres) for MP 18 and MP 20 match the beam paths in Fig. 4 on the top.

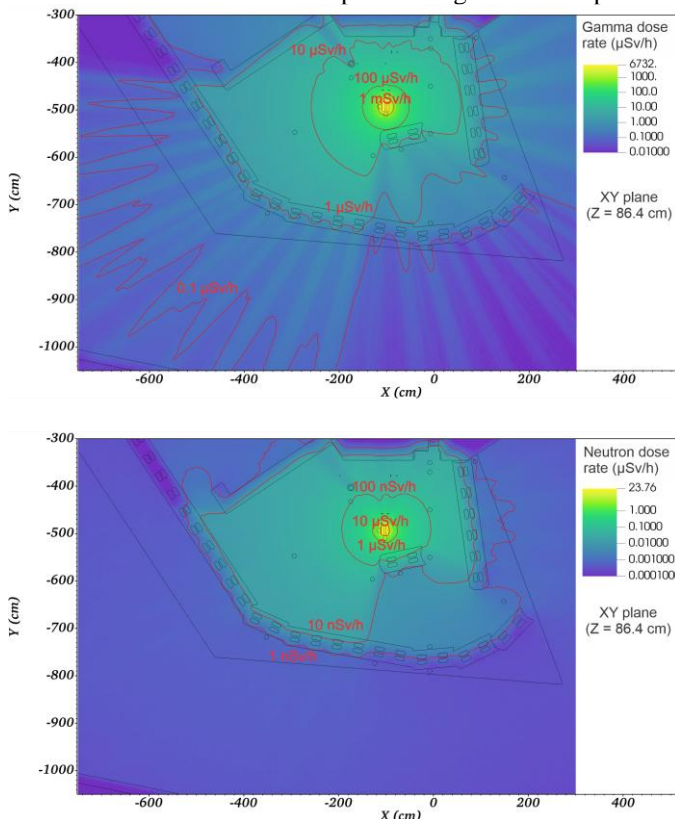


Fig. 4. Calculated global gamma (top) and neutron (bottom) $H^*(10)$ dose rate field around KATANA using a single source location of activated water (Snail No. 1) in a horizontal cross-section view (Configuration 1, flow rate 0.4 L/s, full reactor power 250 kW). Contour lines are shown in red.

Results of the calculated gamma and neutron dose rate at locations of the 21 MPs throughout the reactor hall are presented in Table II. The relative uncertainty, which only takes into account the statistical uncertainty of the Monte Carlo simulation, is well below 1% for the majority of MP and up to

2% for those outside the concrete wall. In addition, the C/E values (calculation vs experiment) are included, whereby experimental data have the stated 25 % measurement uncertainty. C/E values between 0.2 - 5 (difference by a factor of 5) are highlighted for better clarity.

The C/E values for gammas are for all MPs below 1 (underestimation), whereby eight of them show a value within a factor of 5 (highlighted). These MPs, in which the contribution from the activated water inside the outer observation Snail No. 1 is the largest, are located in the immediate vicinity of the source (MP 13 and MP 14) or are located behind the shielding wall. Results for other MPs differed even more due to the higher contribution of the activated water from the remaining part of the circuit.

The C/E results for neutrons show an even larger deviation, although C/E values for MPs outside the wall are not available due to extremely low (not measurable) dose rate values. A really good agreement and a slight overestimation (less than a factor of 1.8) are observed near the source (MP 13 and MP 14). Extremely large deviations, underestimation up to a factor of 300, are observed for MPs: [0, 1, 2, 3 and 6]. However, this deviation can easily be neglected since all these MPs are in direct line of sight to the RPP and the primary contribution to the total neutron dose rate originates from the neutrons emitted by the reactor core (which scatter along the empty instrumentation pipe of the inner part of KATANA) rather than from those produced by activated water (^{17}N).

C. Computational results: double source location

The C/E values indicate that in some areas, the contribution of the activated water from the remaining part of the circuit is not negligible and must be taken into account as well. The second most relevant component in the circuit (besides Snail No. 1) is the pump with the high water volume (estimated at 4 litres). To further improve the C/E values, an additional global dose field rate calculation was performed using a double source location of activated water, i.e. inside Snail No. 1 and the pump. The source intensity for the pump was determined on a similar basis as for the Snail, i.e. calculated saturated activity, considering a longer decay/transfer time (the pump is located further along the circuit) and a larger water volume as: $3.99 \times 10^7 \text{ Bq}$ (^{16}N : 64.291 %), $3.54 \times 10^3 \text{ Bq}$ (^{17}N : 0.008 %) and $1.05 \times 10^7 \text{ Bq}$ (^{19}O : 35.701 %).

The results of the global γ (top) and neutron (bottom) dose field distributions around KATANA, based on a double source location of activated water (Snail No. 1 and the pump), are presented in Fig. 5 (horizontal cross-section: XY plane at $Z = 86.4 \text{ cm}$) and Fig. 6 (vertical cross-section: XZ plane at $Y = -493 \text{ cm}$, corresponding to the centre of Snail No. 1), with contour lines included for improved clarity. The impact of the second source, i.e. the pump, is not negligible, as increased dose rates can be clearly observed by the outward shift of the contour lines from both sources. This effect is particularly evident in areas closer to the pump or in regions that were previously well shielded from Snail No. 1 but are now in direct line of sight from the pump. In addition, the calculated relative statistical uncertainties of the global meshtally distribution for neutrons

and gammas are provided on the right side in Fig. 5 and Fig. 6. The relative statistical uncertainty is both for neutrons and gammas practically below 1 % inside the experimental area and below 5 % in the remaining reactor hall. However, the reader should be aware that these are only statistical uncertainties of

the Monte Carlo simulation whereby uncertainties of the RRs, geometry, etc. are not yet included. This will be an important aspect to evaluate for the future work.

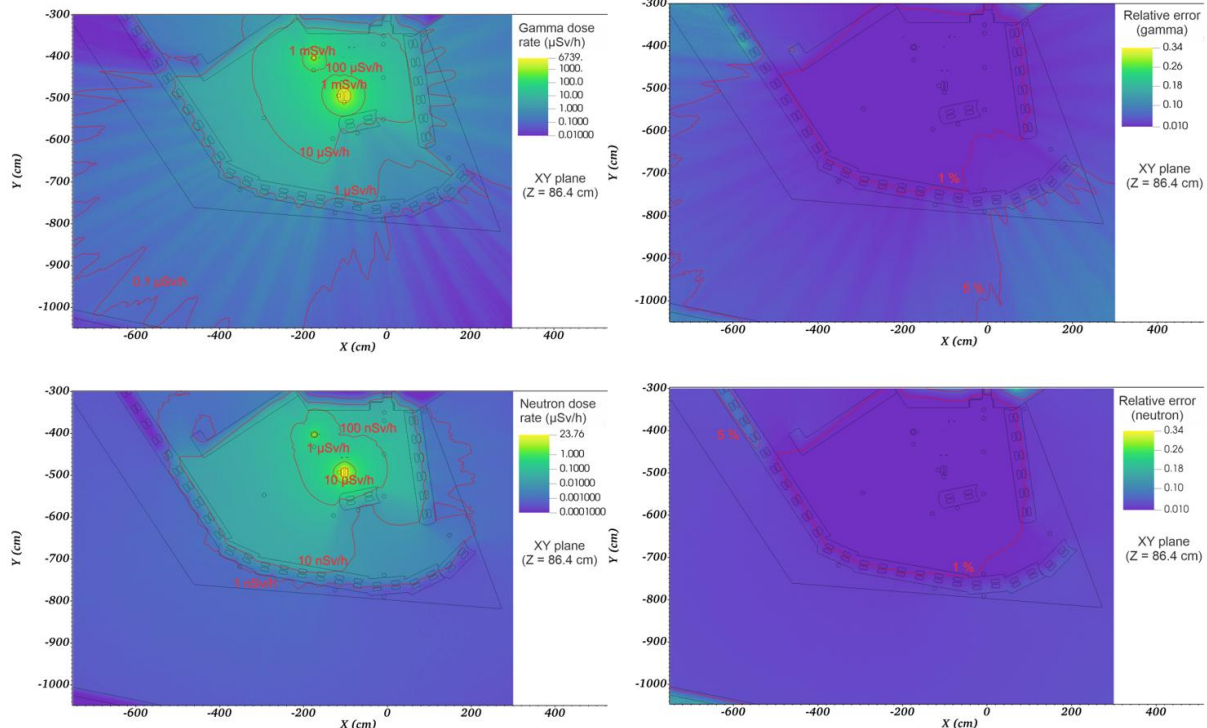


Fig. 5. Calculated global gamma (top) and neutron (bottom) $H^*(10)$ dose rate field around KATANA using a double source location of activated water Snail No. 1 + pump) in a horizontal cross-section view (Configuration 1, flow rate 0.4 L/s, full reactor power 250 kW). Contour lines are shown in red.

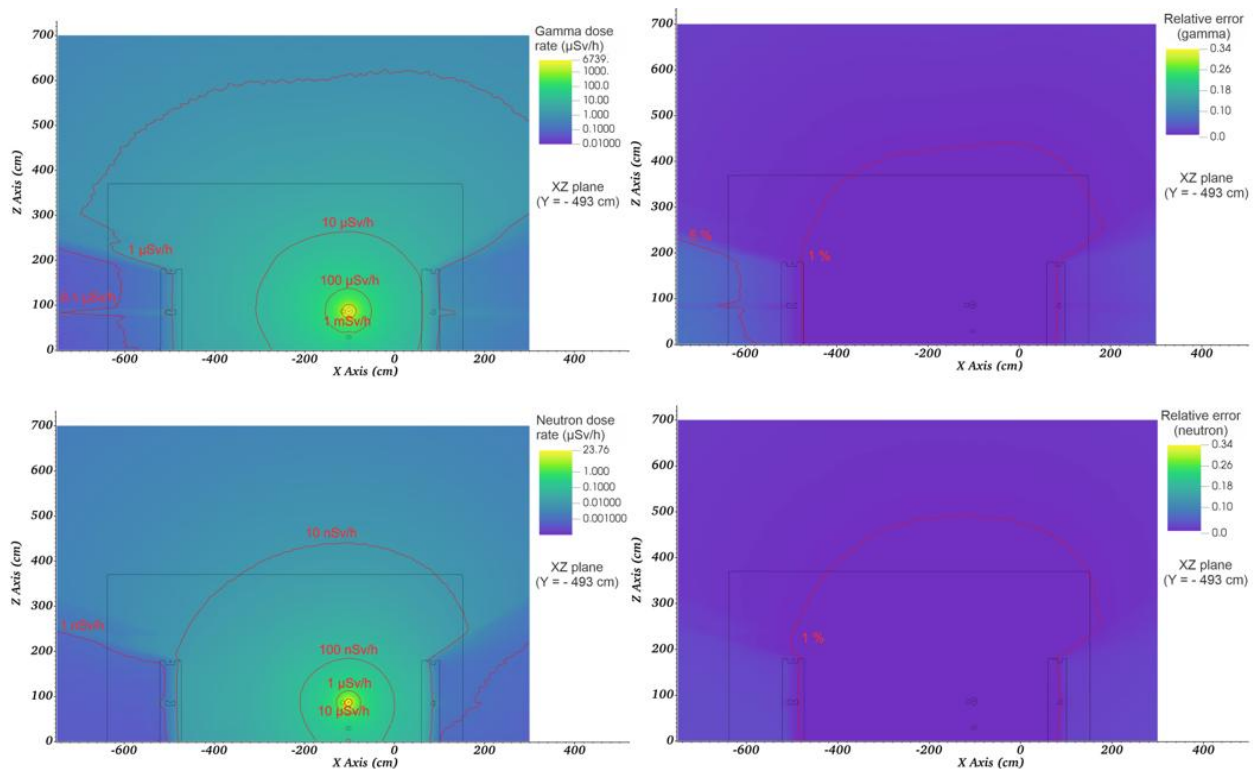


Fig. 6. Calculated global gamma (top) and neutron (bottom) $H^*(10)$ dose rate field around KATANA using a double source location of activated water Snail No. 1 + pump) in a vertical cross-section view (Configuration 1, flow rate 0.4 L/s, full reactor power 250 kW). Contour lines are shown in red.

Furthermore, results at the dedicated MPs, using both sources (Snail No. 1 and the pump), are presented in Table II as well. Improvement of C/E values is observed, especially at MPs near the pump, i.e. MP: 15, 16, 5, 18 and 20. Results indicate that considering the extra source of the activated water leads to the right path towards C/E being closer to unity (resulting in a higher number of highlighted values).

V. CONCLUSION

For radiological safety assessment, gamma and neutron dose rates were measured around the KATANA facility during steady-state operation of the JSI TRIGA reactor at full power. The highest gamma dose rate, reaching up to 5 mSv/h, was measured near the main observation part of the circuit, i.e. outer Snail no. 1 – short loop, with an additional local increase near the pump attributed to the higher water volume in that area. Outside the concrete shielding labyrinth, however, dose rates remained below the regulatory limit of 10 μ Sv/h, indicating that no further shielding is necessary. The neutron contribution to the total dose rate was significantly lower—more than three orders of magnitude lower compared to gamma contribution.

In addition, experimental results were supported with the calculations using a simplified convectional method excluding detailed fluid dynamics. A comparison between calculated and experimental (C/E) results revealed that gamma dose rates were underestimated by a factor of 2 to 5, while neutron dose rates near the primary source (Snail No. 1) were overestimated by a factor of 1.8. Including the pump as a secondary source improved agreement between simulation and measurement, emphasizing the need for accurate source modelling.

The C/E comparison of the dose rate values provided valuable insights into the water activation analysis of the KATANA facility and highlighted both the complexity and the challenges of carrying out such an absolute comparison. Further work, in particular the implementation of the use of state-of-the-art fluid activation codes (such as RSTM, FLUNED, GammaFlow & ActiFlow) to more precisely define and implement the distribution of activated water not only within the Snail No. 1 and the pump but also throughout the rest of the circuit and/or different loop configuration (Configuration 1, 2 or 3). In addition, such codes also allow for a more detailed source modelling, so that a mesh-based source distribution can be defined more correctly along the Snails (so far, the source has been distributed uniformly over the entire water volume of the Snail or the pump, thus implementing an additional simplification/uncertainty to the model).

Furthermore, additional research and the improvement of experimental results (either by using dose rate detectors with lower measurement uncertainty or by measuring the neutron and gamma flux with absolutely calibrated neutron and gamma detectors which have much lower uncertainty, i.e. HPGe) are extremely important and an essential part towards the goal of performing benchmark quality experiments at KATANA with a well-defined and low experimental and computational uncertainty.

ACKNOWLEDGMENT

The authors acknowledge the support of the Slovenian

Ministry of Education, Science and Sport (project codes P2-0405 Fusion technologies; P2-0073 Reactor physics; PR-12326/PR-12842, Training of young researchers, NC-0022 Water activation in nuclear reactors). This work has been carried out within the framework of the EUROfusion Consortium, funded by the European Union via the Euratom Research and Training Programme (Grant Agreement No 101052200 — EUROfusion). Views and opinions expressed are, however, those of the author(s) only and do not necessarily reflect those of the European Union or the European Commission. Neither the European Union nor the European Commission can be held responsible for them.

REFERENCES

- [1] A. Žohar, L. Snoj, "On the dose fields due to activated cooling water in nuclear facilities," *Prog. Nucl. Energy*, vol. 117, 2019, Art. no. 103042. <https://www.sciencedirect.com/science/article/pii/S0149197019301374>
- [2] N. ITER organization ITER, homepage (2024). Available: <http://www.iter.org>. Accessed on: 1.7.2025
- [3] X. Litaudon et al., "Eurofusion contributions to iter nuclear operation," *Nuclear Fusion*, 2024
- [4] D. Kotnik, A.K. Basavaraj, L. Snoj, I. Lengar, "Design optimization of the closed-water activation loop at the JSI irradiation facility," *Fusion Eng. Des.*, vol. 193, 2023, Art. no. 113632. [Online]. Available: <https://www.sciencedirect.com/science/article/pii/S0920379623002168>
- [5] Domen Kotnik, Julijan Peric, Domen Govekar, Luka Snoj, Igor Lengar, "KATANA water activation facility at JSI TRIGA, Part I: Final design and activity calculations," *Nucl. Eng. Technol.*, 2024. [Online]. Available: <https://doi.org/10.1016/j.net.2024.09.036>
- [6] . Peric and D. Kotnik, "KATANA: webpage," 2024. Accessed: 2025-07-22.
- [7] L. Snoj, D. Kotnik et al., A Half-Century of Nuclear Research, Education and Training: Story of the JSI TRIGA Reactor, *Annals of Nuclear Energy* (2025). <https://doi.org/10.1016/j.anucene.2024.111122>
- [8] J. Peric, D. Kotnik, L. Snoj, V. Radulović, Neutron emission from water activation: Experiments and modeling under fusion-relevant conditions at the KATANA facility, *Fusion Engineering and Design*, Volume 216, 2025, <https://doi.org/10.1016/j.fusengdes.2025.115052>.
- [9] R. Pampin, E. Masia, F. Cau, D. Kotnik, R. Villari, A. Portone, Insights from applications of the RSTM tool for coupled CFD-activation fluid simulation, *Fusion Engineering and Design*, Volume 203, 2024, <https://doi.org/10.1016/j.fusengdes.2024.114466>.
- [10] Eduardo Masiá, et. al., Application of the radio species transport model to the JSI water activation loop, *Fusion Engineering and Design*, Volume 219, 2025, <https://doi.org/10.1016/j.fusengdes.2025.115264>.
- [11] M. De Pietri, J. Alguacil, E. Rodríguez and R. Juárez, Development and validation in water of FLUNED, an open-source tool for fluid activation calculations, *Computer Physics Communications* 291, 108807 (2023). <https://doi.org/10.1016/j.cpc.2023.108807>
- [12] T. Berry, C. Nobs, A. Dubas, R. Worrall, T. Eade, J. Naish and L. Packer, Integration of fluid dynamics into activation calculations for fusion, *Fusion Engineering and Design* 173, 112894 (2021). <https://doi.org/10.1016/j.fusengdes.2021.112894>
- [13] D. Govekar, J. Peric, D. Kotnik, V. Radulovic. Calibration of HPGe detectors and usage of prompt gamma rays to extend detector efficiency curve in above 2 MeV range.
- [14] EUROfusion, "The demonstration power plant: DEMO", <https://euro-fusion.org/programme/demo/>, (2024), accessed: 2025-05-06.
- [15] D. Brown, et.al., ENDF/B-VIII.0: The 8th Major Release of the Nuclear Reaction Data Library with CIELO-project Cross Sections, New standards and Thermal Scattering Data, *Nuclear Data Sheets* 148, 1 (2018), special Issue on Nuclear Reaction Data.
- [16] J. García, J. P. Catalán and J. Sanz, Development of the automatic void generation module in GEOUNED conversion tool, *Fusion Engineering and Design*, 168, 112366 (2021).
- [17] ICRP, Data for Protection Against Ionizing Radiation from External Sources: Supplement to ICRP Publication 15, ICRP Publication 21 (Pergamon Press, Oxford, 1973).
- [18] H. Rossi et al., Protection against neutron radiation, NCRP-38, National Council on Radiation Protection and Measurements (1971).